Multi-organ Statistical Shape Model Building Using a Non-rigid ICP Based Surface Registration

Jiaqi Wu
Graduated School of Engineering, Kyushu Institute of Technology, Kitakyushu, Japan
Email: wujiaqi_alan@outlook.com

Guangxu Li
School of Electronics and Information Engineering, Tiangong University, Tianjin, China
Email: liguangxu@tiangong.edu.cn

Tohru Kamiya
Kyushu Institute of Technology, Kitakyushu, Japan
Email: kamiya@cntl.kyutech.ac.jp

***Abstract*—Landmark correspondence is one of the key steps in Statistical Shape Model (SSM) building. In this paper, a non-rigid iterative closest point surfaces registration method is introduced to seek proper corresponded landmarks in the multi-organ surface meshes. Surfaces of four abdominal organs are used in the experiment to build SSM from landmarks corresponded by five different registration strategies. The proposed method of individually non-rigid registration of single organs shows the least errors measured by Hausdorff distance and the best model quality of generalization ability, specificity, and compactness.**

***Index Terms*—multi-organ, statistical shape model, surface registration, landmark correspondence**

I. Introduction

Statistical Shape Model (SSM) is a widely developed and applied tool for medical image analysis tasks, including segmentation, reconstruction of object organs or tissue [1], [2]. The processed data and information in SSM can be used in Computer-Aided Diagnosis (CADx), surgical planning and navigation, medical education, and so on fields. The SSM is composed of Point Distribution Models (PDM), where the deformation patterns of the object shape are learned from the special varieties of corresponding landmarks in a group of aligned meshes represented by vertices and faces in a training set. The landmarks are a certain number of vertices picked from each of the dense surface meshes from different patients, which represent vertices with the same anatomic structure of shape. The correspondence of landmarks is an essential procedure in the SSMs building to accurately extract the information of variation in the surface mesh data. Although manually landmark corresponding is realizable for two-dimensional (2-D) shapes with a limited number of vertices and cases, it is difficult to find corresponding landmarks from three-dimensional (3-D) surfaces due to the increasing quantity of candidate vertices and complexity of the geometric shape. Thus, automatic correspondence methods are more favorable for relevant tasks.

The problem of landmark correspondence can be cast as a combination of shape correspondence and landmark prototype building. The correspondence of shapes is usually stated as a problem of finding proper mappings between their elements (ordinarily vertices) and referred to as registration, alignment, or matching problems [3], [4]. According to the completeness of the mapping, i.e., whether a full correspondence for each of the elements from the moving shape to the fixed shape is required, the correspondence problem can be classified into dense correspondence or sparse correspondence. The difficulties are almost the same because the searching space still covers the whole shape to find proper and meaningful correspondence, to ensure the quality of SSM built.

A fundamental distinguishment of the shape registration methods is the form of deformation, which can be roughly classified as rigid or non-rigid registration. The geometric deformation that matches one shape to another is differently chosen when adapted to shapes from different sources or for different tasks. One of the typical applications of rigid registration is the surface reconstruction from multiple point clouds partially scanned in different viewpoints of an identical object. Since the surfaces to be aligned are obtained from one object, only rigid deformation, i.e., translation, orientation, and scale are required in consideration. In rigid registration problems, noise, outlier, and the limited amount of overlapping are the main difficulties [5]. However, in the scope of biomedical surfaces, surface meshes are generated from medical images obtained from different

Manuscript received December 13, 2021; revised June 10, 2022.

doi: 10.18178/joig.10.3.95-101

patients, and some of the conditions and characteristics of the object surfaces are distinctive from those of ordinary surfaces. Thus, rigid deformation is not enough to describe the deformation of the organs or tissue surfaces and non-rigid registration is required to match the surfaces of individual differences.

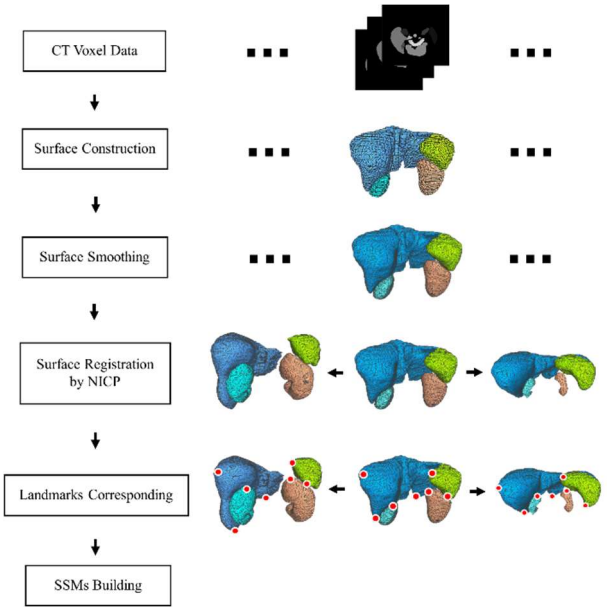

Figure 1. Flow chart of the proposed architect of NICP-based landmark corresponding and SSMs building.

Davies *et al.* [6] proposed an automatic landmark corresponding method that used the Minimum Description Length (MDL) principle to find the optimal parameterization of training shape. Three properties of the built shape model: generalization ability, specificity, and compactness are introduced as quantitative measures of model quality. In our previous research [7], the correspondence of landmarks is conducted across parameterized surfaces obtained from spherical conformal mapping and Demon registration. The parameterization that maps each of the original surfaces in the training set to spherical surfaces decreases the complexity of finding identity landmarks while preserving relevant information among vertices in the original organ surfaces to a certain extent. After a dense matching of the whole training set, landmarks with geometrical and anatomical representativeness are chosen from the original surface. In our previous methods, surface simplification using quadric error metrics and k-means clustering is implemented in one of the original surface mesh in the training set to obtain a set of reference landmarks. Ravikumar *et al.* [8] introduce a group-wise similarity registration using Student's t-mixture model for landmarks corresponding.

In the field of medical image analysis, more attention is paid to multi-organ models instead of organ-, and disease-specific methods [9]. The combination of inter-organ relations, including spatial, functional, and physiological relations, provides more accurate human anatomy information and benefits many medical procedures, including diagnosis, therapeutic assistance, radiotherapy planning, surgery simulation, or injury severity prediction. However, the jointed structure of multiple organ surfaces is unable to be parameterized into one single surface and the following spherical registration could not be conducted. Therefore, to extend our SSM building scheme and make it available for multi-organ models, a non-parameterization-based registration method is introduced and applied in the proceeding of landmark correspondence.

In the paper, a non-rigid iterative closet point method is introduced for automatic surface registration of 3-D multi-organ surface meshes. Different strategies of single organ and multi-organ combination are compared in the registration scheme on four abdominal organs from different patients.

II. Method

In our research, a Non-rigid Iterative Closest Point (NICP) method is applied to landmark correspondence for multi-organ SSMs building from 3-D volume data of medical images. The flow chart of the proposed architect is shown in Fig. 1. In the first step, a series of preprocesses are necessary to obtain suitable surface meshes for landmarks correspondence from medical images. A marching-cubes algorithm is applied to the manually segmented voxel data, which is a process that transformed the labeled medical image of organs to triangular surface meshes. The following surface filtering is performed to improve the smoothness of the transformed rough surfaces. To decrease the computational amount of the following processes on surface meshes, a surface simplification algorithm is applied on the smoothed organ meshes. In the second step, a reference mesh of landmarks is prepared by a k-means clustering procedure which is performed on a chosen surface. Then, the chosen surface is regarded as the target surface and the other surfaces in the rest of the training set are registered to it. The landmarks of the other cases can be corresponded by finding the nearest vertices on the target surface from the deformed surfaces. After the correspondence, an SSM can be generated from the aligned landmarks by principal component analysis (PCA). A series of surface deformation patterns are learned from the set of landmarks of human organ surfaces.

A. Construction of Surface Data

In our research, the original data of multiple organs are obtained from manually labeled CT (computed tomography) scans by experts. In the 3-D CT images, the organs are expressed by connected cubic voxels. To extract the surface of organs, the Marching Cubes (MC) algorithm is applied to the labeled voxels. In the algorithm using the divide and conquer strategy, eight pixels from two adjacent slices form a cube and the key is to find a surface intersection in the cube. 14 patterns from all 256 cases of possible intersection ways are precalculated to approximate the linear interpolations and output the triangular surface meshes. The algorithm traversed all cubes and produces a triangular surface mesh. For multiple organs, the marching cubes are performed organ by organ to avoid merging extremely closing organs to one the same surface.

As the original data from medical images are obtained from the imaging system under certain resolutions, the

naturally smoothing human organs and tissues are inevitably transformed to discrete voxels data and the discreteness remains in the triangular surfaces obtained from the MC algorithm. To decrease the roughness of the surface and recover the smoothness in general, a Gaussian filter is applied to the surfaces. The smoothing procedure can also remove the noise of cube edges and benefic the following registration procedures. In surface registration, the similarity is a basis to find the correspondence. However, some of the similarities in local voxel structures are produced from the MC algorithm but not from the original anatomical features of human organs. The smoothing can reduce the effect of the MC and restore the basic anatomical contours of the organs.

Although the quality of the surfaces is improved in the smoothing procedure, the quantity of vertices and faces on the surface remains the same and it is more than required. The vertices originated from MC are generated cube by cube and redundant vertices that describe the same geometry structures can be simplified to decrease the computational amount of the following processes on surface meshes. Thus, a quadric matrices surface simplification algorithm that can rapidly approximate the original surface is applied to the smoothed organ meshes.

B. Generation of Landmarks Prototype

Before the registration and correspondence, it is necessary to prepare a set of standard landmarks. A set of ideal landmarks should be representative of the anatomical structure of the object organ surface with a small ratio of the vertices and faces in the original surface. Also, as the final aim of landmark corresponding is to build an SSM, it is important to capture the varieties that existed in the identical positions of landmarks from different patients. A set of satisfied reference landmarks is the first step of building an SSM of high quality.

First, one of the surface cases is randomly chosen from the training set of surface meshes obtained before. Then, a k-means clustering based surfaces simplification method proposed in our previous research [7] is performed to extract representative vertices from the chosen surface as the reference landmarks. Given a required number of landmarks k and a surface with n vertices, for each of the vertices, a set of spatial and geometrical feature vector $\boldsymbol{v}$ is extracted, and the vertices are divided into k clusters as $\boldsymbol{D} = \{D_1, D_2, \dots, D_k\}$ with $\boldsymbol{c}_i$ the center of the ith cluster. The clustering is equal to find a stable division $\boldsymbol{D}$ with minimal Within-Cluster Sum of Squares (WCSS):

$$\arg\min_{\boldsymbol{D}} \sum_{i=1}^{k} \sum_{\boldsymbol{v}\in \boldsymbol{D}_i} \|\boldsymbol{v} - \boldsymbol{c}_i\|^2 \quad (1)$$

In the initial step of the algorithm, a set of k initial clustering centers is chosen, and an initial clustering is obtained by Voronoi diagram division. Then the algorithm turns into iterations where new centers $\boldsymbol{c}$ are updated by the new divisions $\boldsymbol{D}$ until it converges (the division is fixed). The finally obtained centroids of the vertices in each of the k clusters are regard as reference landmarks. The faces of the landmarks could be generated by spherical Delaunay triangulation which is performed on the sphere mapped from the chosen surface mesh. The landmarks from clustering-based simplification method possess better global representativeness, compared with local surface simplification methods, due to the operation of clustering is applied to all vertices at the same time within each iteration.

C. Registration and Correspondence

Surfaces in the training set are extracted and reconstructed from CT images acquired from different patients and the sates of body positions, which produces large diversity of identical organ and tissues and makes landmarks corresponding more difficult. Such differences could not be described and deformed within rigid registration and non-rigid surface registration method is required. In this paper, we introduce a NICP registration to match surfaces to the chosen reference surface throughout the training set.

Given two points sets $\boldsymbol{P}^s = \{\boldsymbol{p}_i^s, i\epsilon 1, \dots, N^s\}$ of N^s vertices and $\boldsymbol{P}^t = \{\boldsymbol{p}_i^t, i\epsilon 1, \dots, N^t\}$ of N^t vertices represent the source mesh and the target mesh respectively, a series of pairwise registration operations is described on them. At first, a rigid Iterative Closest Point (ICP) algorithm using Nearest Neighbor (NN) are searched in the iterations. For each vertex $\boldsymbol{p}_i^s$ in the source mesh, one forward corresponding vertex and one or more backward corresponding vertex (vertices) can be corresponded in the target mesh. The bidirectional displacements from the vertices to each corresponding vertex of forward and backward are used to find rigid transforms of translation, rotation and scaling and get the new displacement $\boldsymbol{\delta}(\boldsymbol{p}_i^s)$. After the rigid registration, a non-rigid deformation from the source mesh to the target mesh is approximated by a sum of N^g Gaussian Radial Basis Functions (G-RBF) with centers $\boldsymbol{c_j}$ and appropriate coefficient $\boldsymbol{\omega}_j$ [10]:

$$r(\boldsymbol{p}_i^s) = \sum_{j=1}^{N^g} \boldsymbol{\omega}_j \rho(\boldsymbol{p}_i^s - \boldsymbol{c_j}) \text{ with } \rho = e^{-(\mu\|\boldsymbol{p}_i^s\|^2)} \quad (2)$$

which is subject to the constraints as:

$$\boldsymbol{\delta}(\boldsymbol{p}_i^s) = \sum_{j=1}^{N^g} \boldsymbol{\omega}_j \rho(\boldsymbol{p}_i^s - \boldsymbol{c_j}), i = 1, \dots, N^g \quad (3)$$

The number N^g is smaller than the vertices in the whole surface. The $\boldsymbol{\omega}_j$ can be solved by minimizing:

$$\sum_{j=1}^{N^g} \|r(\boldsymbol{p}_i^s) - \boldsymbol{\delta}(\boldsymbol{p}_i^s)\|^2 + \varepsilon\|\boldsymbol{c}\|^2 \quad (4)$$

The additional Tikhonov L2-regularization term $\varepsilon\|\boldsymbol{c}\|^2$ is introduced in case of instability or ill-condition situations. The optimal deformation coefficients $\boldsymbol{\omega}.$ are obtained given displacement $\boldsymbol{\delta}(\boldsymbol{p}.)$:

$$\boldsymbol{\omega}. = (\boldsymbol{\theta}^T\boldsymbol{\theta} + \varepsilon\boldsymbol{I})^{-1}\boldsymbol{\theta}^T\boldsymbol{\delta}(\boldsymbol{p}.) \text{with } \theta_{i,j} = \rho(\boldsymbol{p}_i^s - \boldsymbol{c_j}) \quad (5)$$

The above registration focuses on single-to-single surface situation and the complexity increases when applied to a multi-organ structure surface. In this structure, the organs are jointed as a whole, and the candidates of deformation are increased as well, which makes the registration more difficult. To verify the feasibility of applying the non-rigid registration algorithm to landmarks corresponding of multiple organs, we designed a series of strategies employing the non-rigid registration to the single or multiple surfaces. The registration can be

performed directly on the multi-organ structure, individually between single organs, or their combination.

D. Statistical Shape Model Building

The SSM is a deformable shape model, where the deformation patterns are learning by statistical analysis from a training set consist of corresponded landmarks. The SSM describes the distribution of vertices of the shape is consist of a mean shape and deformations upon the mean shape. When applied to image segmentation tasks, the SSM is introduced as Active Shape Model (ASM), and an Active Appearance Model (AAM) that describes the density feature around the vertices of the model is required to guide the deformations by matching the model to the images via the appearance feature. In this research, we focus on the building of multi-organ SSMs from the corresponded landmarks.

An initial alignment of the training shapes is required to remove the global linear difference of translation, rotation and scaling among the shapes by the Procrustes analysis. This process concentrates the shapes obtained from different images to a unified space and helps preserve the actual varieties of shape counters instead of their spatial distribution in the images.

In the training set of SSMs containing N instances, the ith landmark shape $\boldsymbol{x}_i$ is composed of n vertices $\boldsymbol{x}_i = (x_{i1}, x_{i2}, x_{i3}, \dots, x_{n1}, x_{n2}, x_{n3})^T \in \mathbb{R}^{3n}$, and the training set is $\boldsymbol{X} = (\boldsymbol{x}_1, \boldsymbol{x}_2, \dots, \boldsymbol{x}_N)$. To capture the deformation patterns, Principal Component Analysis (PCA) is employed to the training set. The mean shape $\bar{\boldsymbol{x}}$ and covariance matrix $\boldsymbol{S}$ is firstly calculated:

$$\bar{\boldsymbol{x}} = \frac{1}{N}\sum_{i=1}^{N} \boldsymbol{x}_i \tag{6}$$

$$\boldsymbol{s} = \frac{1}{N-1}\sum_{i=1}^{N} (\bar{\boldsymbol{x}} - \boldsymbol{x}_i)(\bar{\boldsymbol{x}} - \boldsymbol{x}_i)^{\boldsymbol{T}} \tag{7}$$

And the eigenvectors $\boldsymbol{\Phi} = (\boldsymbol{\phi}_1, \boldsymbol{\phi}_2, \dots, \boldsymbol{\phi}_m)$ and their corresponding eigenvalues $\boldsymbol{\lambda} = (\lambda_1, \lambda_2, \dots, \lambda_m)$, where $m = \max((s-1), 3n)$. The eigenvalues are sorted and the largest c eigenvalues and eigenvectors are retained to move noise of the data. A proportion δ (usually ranged from 0.95 to 0.995) is used to obtain C by:

$$\sum_{i=1}^{C} \lambda_i \geq \delta \sum_{i=1}^{m} \lambda_i \tag{8}$$

III. Experimental Result

A. Data Preparation

In the experiment, 30 cases of manually labeled 3-D volume data of human abdominal organs are included in the training from the "Multi-atlas labeling beyond the cranial vault-workshop and challenge". Four of the organs: the spleen, right kidney, left kidney, and liver is regarded as basic single organ element of the multi-organ SSMs. The rest of the labeled organs are remarked as background. The surfaces of the organs are generated from the volume data using the surface reconstruction method mentioned in Section II.A. 30 cases of surface mesh under four simplification levels are used in the registration.

B. Surface Registration

The registration of multiple surfaces can be merged into one joint surface or decomposed into matchings between surfaces of single organs. To verify the effectiveness of NICP performed on multi-organ structures, five surface registration strategies are implemented in the experiment. In method 1, the classical rigid ICP is performed to the jointed multi-organ surface, which is also a basic step among all the rest methods. In method 2, a NICP described in [10] is directly performed to the multi-organ structure. In method 3, after rigid ICP registration, a NICP registration is firstly applied to the multi-organ structure and the single organs are individually registered. The flow in method 4 is similar to method 3, except for the procedure, where single organ registration is advanced before multi-organ. In method 5, only single organ registration is retained after the global rigid ICP.

Another variate is the simplification level of the surfaces. The deeper the simplification is, the fewer vertices left, and fewer computing resources are required. We prepared four simplification level $\alpha \in \{1,2,3,4\}$, which retains a ratio of $2^{-(\alpha-1)}$ vertices after the simplification.

To evaluate the registration result, the Hausdorff distance is introduced in the paper. Given two pointsets $\boldsymbol{A} = \{\boldsymbol{a_1}, \boldsymbol{a_2}, \dots, \boldsymbol{a}_{N_a}\}$ and $\boldsymbol{B} = \{\boldsymbol{b_1}, \boldsymbol{b_2}, \dots, \boldsymbol{b}_{N_b}\}$, the one-sided Hausdorff distance from $\boldsymbol{A}$ to $\boldsymbol{B}$ is defined as:

$$\tilde{\xi}_H(\boldsymbol{A}, \boldsymbol{B}) = \max_{a \in \boldsymbol{A}} \min_{b \in \boldsymbol{B}} \|\boldsymbol{a} - \boldsymbol{b}\| \tag{9}$$

And the bidirectional Hausdorff distance between A and B is defined as:

$$\xi_H(\boldsymbol{A}, \boldsymbol{B}) = max(\tilde{\xi}_H(\boldsymbol{A}, \boldsymbol{B}), \tilde{\xi}_H(\boldsymbol{B}, \boldsymbol{A})) \tag{10}$$

The Hausdorff distance measures the maximum of the distances from each point in A to the closest point in B.

The five registration strategies described before were applied to the training set of 30 abdominal multi-organ surfaces under four simplification levels. The case of reference surface used in Section II.C was regarded as the target surface and the rest 29 cases of surfaces in the training set were registered to the target surface. The mean Hausdorff distance of the registration pair is shown in Table I.

The comparison of simplification levels under the same method shows that the simplification levels only have a negligible effect on the registration results. The introduction of non-rigid registration enormously increases the accuracy of registration. Compared with the former methods, the independent registration of single organs in method 4 deforms the surfaces to individual organs before mapping them to the wrong organs in the multiple organ structures and increases the accuracy. In method 5, using more iteration of NICP of single organs instead of multi-organ level registration also increases the registration result.

TABLE I. MEAN ACCURACY AND SPECIFICITY

Hausdorff Distance	SL 1	SL 2	SL 3	SL 4
Method 1	21.44±6.36	21.26±6.31	21.12±6.25	21.12±6.25
Method 2 [10]	16.26±5.72	15.74±5.44	15.24±5.3	14.62±4.91
Method 3	16.24±7.40	15.55±7.34	14.97±7.17	14.89±6.55
Method 4	13.68±6.44	13.26±6.25	13.34±5.99	13.68±5.86
Method 5	12.37±6.20	11.92±5.90	11.73±5.50	12.00±5.47

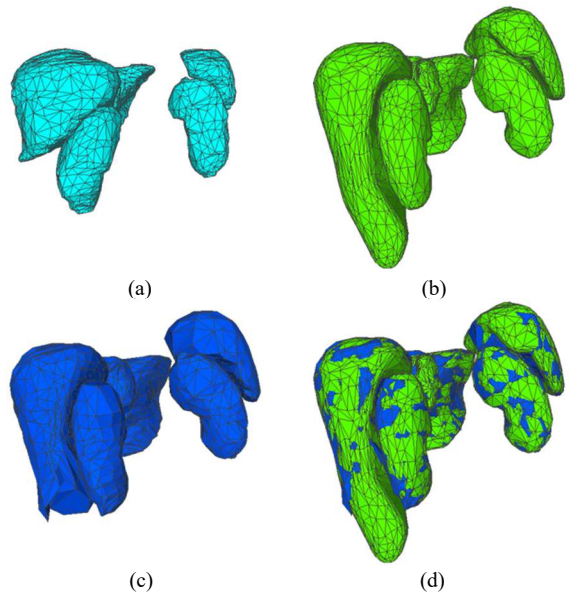

Figure 2. One example of registration results with large Hausdorff distance: four surfaces representing (a) source mesh, (b) target mesh, (c)deformed mesh, and (d) a combination of target mesh and deformed mesh. The order of organs shown in each surface is: liver, right kidney, left kidney, and spleen.

Although the Hausdorff distance of registration is improved by introducing the NICP algorithm, some cases of the registration results yield bad matching which may lead to negative effects to the SSMs. An example of registration results with a Hausdorff distance of 28.15 is shown in Fig. 2. By comparing the source mesh (cyan), the target mesh (green), and the moved source mesh (blue), a large difference after registration can be found in the bottom region of the liver organ.

C. Shape Model Building

The SSMs were generated from the landmarks that corresponded from the registration of multi-organ surfaces simplified in level 2. To evaluate the quality of SSMs built from the landmarks obtained by five different registration methods, three benchmarks of model quality, namely generalization ability, specificity, and compactness, are introduced in the experiment.

The first property of an SSM is the generalization ability which is the ability to construct new instances out of the training set, as well as the ability to avoid over fittings. Generating new shapes is a vital ability in the application of SSM. Suppose M is the number of modes used to build the model for fitting the current instance that is not included in the training set as much as possible. Suppose the number of instances inside the training set is t, the generalization ability $G(M)$ is expressed as:

$$G(M) = \frac{1}{t}\sum_{i=1}^{t}|\boldsymbol{y}_i - \boldsymbol{y}_i'(M)|^2 \quad (11)$$

where shape $\boldsymbol{y}_i$ denotes the excluded instance and shape $\boldsymbol{y}_i'(M)$ denotes the instance that best fitted to $\boldsymbol{y}_i$ using the former M modes of the SSM.

To compare the generalization ability $G_P(M)$ and $G_Q(M)$ of two models P and Q, when $G_P(M) \leq G_Q(M)$ is satisfied for all of the M and $G_P(M) < G_Q(M)$ is satisfied for some of the M, then the model P is considered better than Q in the aspect of generalization ability.

The second property, specificity, reflects the ability of generating shapes which are similar to those included in the training set, which is expressed as:

$$S(M) = \frac{1}{t}\sum_{i=1}^{t}|\boldsymbol{y}_i(M) - \boldsymbol{y}_i'|^2 \quad (12)$$

where $\boldsymbol{y}_i$ is the shape generated by the model with t eigenvalues on M modes and $\boldsymbol{y}_i'$ is the most approximate shape to $\boldsymbol{y}_i(M)$ in the training set. Similarly to the comparison rules of generalisation ability, for model P and model Q with their specificity $S_P(M)$ and $S_Q(M)$, when $S_P(M) \leq S_Q(M)$ is satisfied for all of the M and $S_P(M) < S_Q(M)$ for some of the M, then the specificity of model P is considered better than that of model Q.

The compactness assesses the ability of constructing the instance with the minimum number of modes possible. Defining λ_i as the ith eigenvalue, the compactness is described by the accumulation of variance:

$$C(M) = \sum_{i=1}^{M}\lambda_i \quad (13)$$

using $C_P(M)$ and $C_P(M)$ to express the compactness of two models P and Q, the comparison rules is like the specificity. The generalization ability, specificity, and compactness of four multi-organ SSMs built from landmarks corresponded using five registration strategies are compared in Fig. 3, Fig. 4, and Fig. 5, respectively.

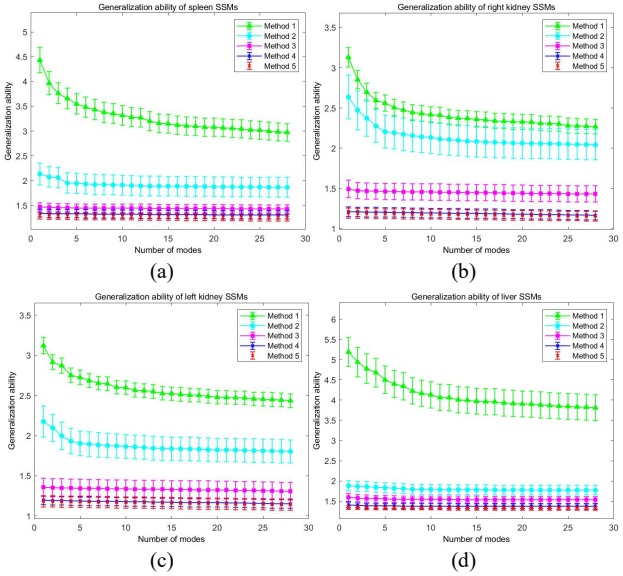

Figure 3. Generalization ability of SSMs built from landmarks corresponded by using for five registration strategies (1: rigid-ICP of multi-organ, 2: NICP of multi-organ, 3: NICP of multi-organ followed by single organs, 4: NICP of single organs followed by multi-organ, and 5: NICP of single organs); (a) Spleen, (b) right kidney, (c) left kidney, (d) liver.

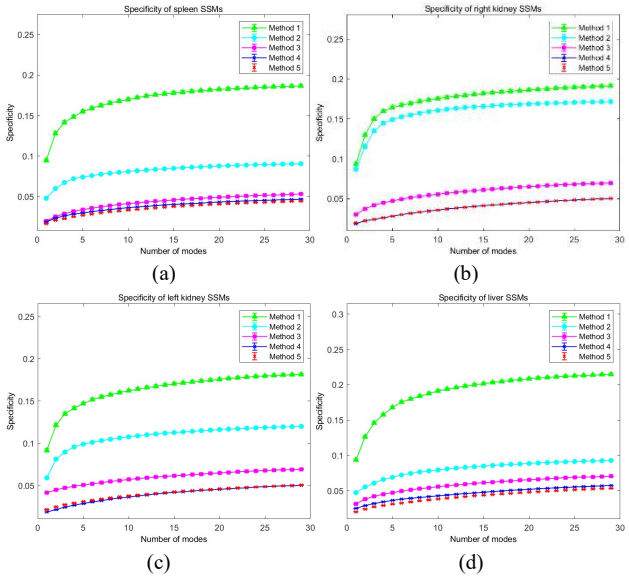

Figure 4. Specificity of SSMs built from landmarks corresponded by using for five registration strategies (1: rigid-ICP of multi-organ, 2: NICP of multi-organ, 3: NICP of multi-organ followed by single organs, 4: NICP of single organs followed by multi-organ, and 5: NICP of single organs); (a) Spleen, (b) right kidney, (c) left kidney, (d) liver.

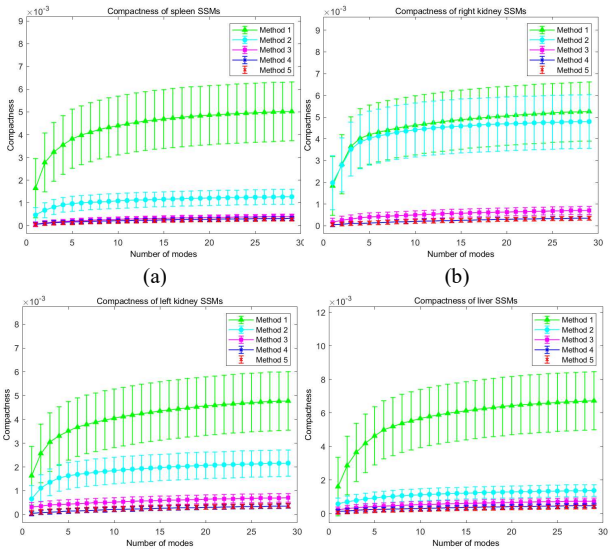

Figure 5. Compactness of SSMs built from landmarks corresponded by using for five registration strategies (1: rigid-ICP of multi-organ, 2: NICP of multi-organ, 3: NICP of multi-organ followed by single organs, 4: NICP of single organs followed by multi-organ, and 5: NICP of single organs); (a) Spleen, (b) right kidney, (c) left kidney, (d) liver.

It can be found that the quality of SSMs built are relative to the registration accuracy in the landmarks corresponding procedure and the model qualities are increasing from method 1 to 5, as the accuracy of registration results. Thus, the introducing of NICP method applied to single-to-single organs registration strategy can benefit the SSMs building process.

IV. Discussion

A. Surface Registration

In the experiments of multi-organ surface registration by using five different methods, the comparison of registration accuracy measured by Hausdorff distance shows that the strategy of method 5, a single organ NICP registration pairs, is more beneficial to the registration accuracy, as shown in Table I.

In method 1, a classic ICP method is performed to the registration of jointed multi-organ structures. The large error in the result shows the necessity of introducing non-rigid transforms for the registration of human organs from different patients so that the deformation space is complex enough to describe the non-rigid distortion among different shapes. In method 2, the jointed surfaces containing four organs are directly matched to the target surface. Although there is no intersection among the four surfaces, as they are constructed from the voxel data of different organs, it is inevitable that some of the organs are anatomically close. In our experiment, the right kidney is posterior to the liver, and the left kidney is posterior to the spleen, which may lead to misregistration when different organs in method 2 are unable to distinguish. The accuracy of surface registration is improved by introducing the NICP, compared to the ICP method, but there is still a problem of misregistration between different organs. In method 3, a single-to-single registration among individual organs is attached after the multi-organ surface registration in method 3. However, the deformation of the surface is misled to the wrong organs in the previous multi-organ surface registration. The strategy of single-to-single registration is unable to fix the problem, which makes the accuracy of method 3 similar to method 2. In method 4, the order of the registration process is adjusted, and the single-to-single registration is brought forward. This operation improved the accuracy by the registration between single organs firstly and alleviates the problem of misregistration among anatomically close organs. In method 5, the registration of multi-organ structures is removed and replaced by a complete single-to-single registration strategy, and this strategy achieves the best result.

Compared with the registration of multi-organ structure, where the four organs are regarded as one united surface, the single-to-single strategy provides additional information of organ category and the misregistration of vertices belonging to different organs is forbidden, which improve the accuracy of the multi-organ registration.

In the experiment, four levels of simplification are performed to the original surfaces which are obtained from the voxel data. The registration accuracy by the same method under different simplification levels is almost the same, which indicates that the simplification rarely affects the registration accuracy. It can be shown that, in process the simplification, the global geometry is nearly not changed despite the number of vertices and faces which are used to describe the surface are decreased rapidly as the simplification level raises. Although the accuracy cannot be improved by simplification, the use of fewer vertices in the registration can improve the efficiency of calculation and reduce the cost of computation resources.

B. SSMs Building

The generalization ability, specificity, and compactness are three indicators to measure the quality of SSMs built from different training sets of landmarks. It also reflects

the effectiveness of the corresponding method. The SSMs of four organs, which are built from the landmarks which are corresponded by using five different registration strategies, are evaluated and their generalization ability, specificity, and compactness are shown in Fig. 3, Fig. 4, and Fig. 5 respectively. The qualities of SSMs built are basically increasing from method 1 to 5 and positively relevant to the accuracy of registration. The SSMs built by using the proposed method of the highest accuracy also possess the highest quality, as the registration is important to the process of finding proper corresponding landmarks on each surface.

V. Conclusion

In this paper, a series of surface registration strategies are applied to the problem of SSMs building. The landmarks are corresponded from the surfaces which are registered by the G-RBF-based NICP method. Different single or multiple organs matching processes are conducted in each of the strategies. The experiment of SSMs building is performed on a training set containing 30 cases of multi-organ surfaces. The result shows that the accuracy of surface registration is improved by the proposed method. Further, the quality of the SSMs is also improved by using the proposed corresponding approach.

Conflict of Interest

The authors declare no conflict of interest.

Author Contributions

Jiaqi Wu conducted the research and wrote the manuscript with support from Guangxu Li and Tohru Kamiya supervised the project and provided suggestion and recommendations along the way. All authors had approved the final version.

References

[1] P. V. Berghe, J. Demol, F. Gelaude, and J. V. Sloten, "Virtual anatomical reconstruction of large acetabular bone defects using a statistical shape model," *Computer Methods in Biomechanics and Biomedical Engineering*, vol 20, pp. 577-586, December 2017.

[2] X. Wang, Y. Zheng, L. Gan, X. Wang, X. Sang, X. Kong, and J. Zhao, "Liver segmentation from CT images using a sparse priori statistical shape model (SP-SSM)," *PloS One*, vol. 12, p. e018524, October 2017.

[3] O. V. Kaick, H. Zhang, G. Hamarneh, and D. Cohen-Or, "A survey on shape correspondence," *Computer Graphics Forum*, vol. 30, pp. 1681-1707, September 2011.

[4] Y. Sahillioğlu, "Recent advances in shape correspondence," *The Visual Computer*, vol. 36, pp. 1705-1721, August 2020.

[5] G. K. L. Tam, Z. Cheng, Y. Lai, F. C. Langbein, Y. Liu, D. Marshall, R. R. Martin, X. Sun, and P. L. Rosin, "Registration of 3D point clouds and meshes: A survey from rigid to nonrigid," *IEEE Transactions on Visualization and Computer Graphics*, vol. 19, pp. 1199-1217, July 2013.

[6] R. H. Davies, C. J. Twining, T. F. Cootes, and C. J. Taylor, "Building 3-D statistical shape models by direct optimization," *IEEE Transactions on Medical Imaging*, vol. 29, pp. 961-981, November 2009.

[7] J. Wu, G. Li, H. Lu, and H. Kim, "Statistical shape model generation using k-means clustering," in *Proc. International Conference on Electronics and Electrical Engineering Technology*, New York, 2018, pp. 207-211.

[8] N. Ravikumar, A. Gooya, S. Çimen, A. F. Frangi, and Z. A. Taylor, "Group-wise similarity registration of point sets using student's t-mixture model for statistical shape models," *Medical Image Analysis*, vol. 44, pp. 961-981, February 2018.

[9] J. J. Cerrolaza, M. L. Picazo, L. Humbert, Y. Sato, D. Rueckert, M. Á. G. Ballester, and M. G. Linguraruf, "Computational anatomy for multi-organ analysis in medical imaging: A review," *Medical Image Analysis*, vol. 56, pp. 44-67, August 2019.

[10] E. A. Audenaert, J. V. Houcke, D. F. Almeida, L. Paelinck, M. Peiffer, G. Steenackers, and D. Vandermeulen, "Cascaded statistical shape model based segmentation of the full lower limb in CT," *Computer Methods in Biomechanics and Biomedical Engineering*, vol. 22, pp. 644-657, March 2019.

Jiaqi Wu received his B.A. degree in Communication Engineering from Shenyang University of Technology, China in 2015 and the M.E. in Electronic and Communication Engineering from Tiangong University, China in 2018. He is currently a Ph.D. student at Kyushu Institute of Technology, Japan. His research focus on multi-organ segmentation from medical images.

Guangxu Li received his doctoral degree of Engineering from Kyushu Institute of Technology, Japan in 2013. He is currently an assistant professor, School of Electronics and Information Engineering, Tiangong University, China. His main works contains medical image processing and its clinical applications; biomedical information detection, especially the field of ophthalmic imaging.

Tohru Kamiya received his B.A. degree in electrical engineering from Kyushu Institute of Technology in 1994, the M.E and Ph.D. degree from Kyushu Institute of Technology in 1996 and 2001, respectively. He is a professor in the Department of Mechanical and Control Engineering at Kyushu Institute of Technology. His research interests are focus on medical application of image analysis. He is currently working on automatic segmentation of multi-organ of abdominal CT image, and temporal subtraction of thoracic CT image sets. He is a member of IEEE, The society of Instrument and Control Engineers of Japan, and The Institute of Electronics, Information and Communication Engineers of Japan.